

## High Pressure ZZ-Exchange NMR Reveals Key Features of Protein Folding Transition States.

Y. Zhang<sup>1,‡</sup>, S. Kitazawa<sup>2,†,‡</sup>, I. Peran<sup>3</sup>, N. Stenzoski<sup>4</sup>, S. A. McCallum<sup>5</sup>, D. P. Raleigh<sup>3,&</sup> and C. A. Royer<sup>1,2,&</sup>

Figure S1.  $^1\text{H}$ - $^{15}\text{N}$  HSQC spectra of CTL9 I98A at 1 bar (red), 300 bar (orange), 450 bar (yellow), 600 bar (green), 900 bar (teal), 1200 bar (blue), and 1500 bar (purple).

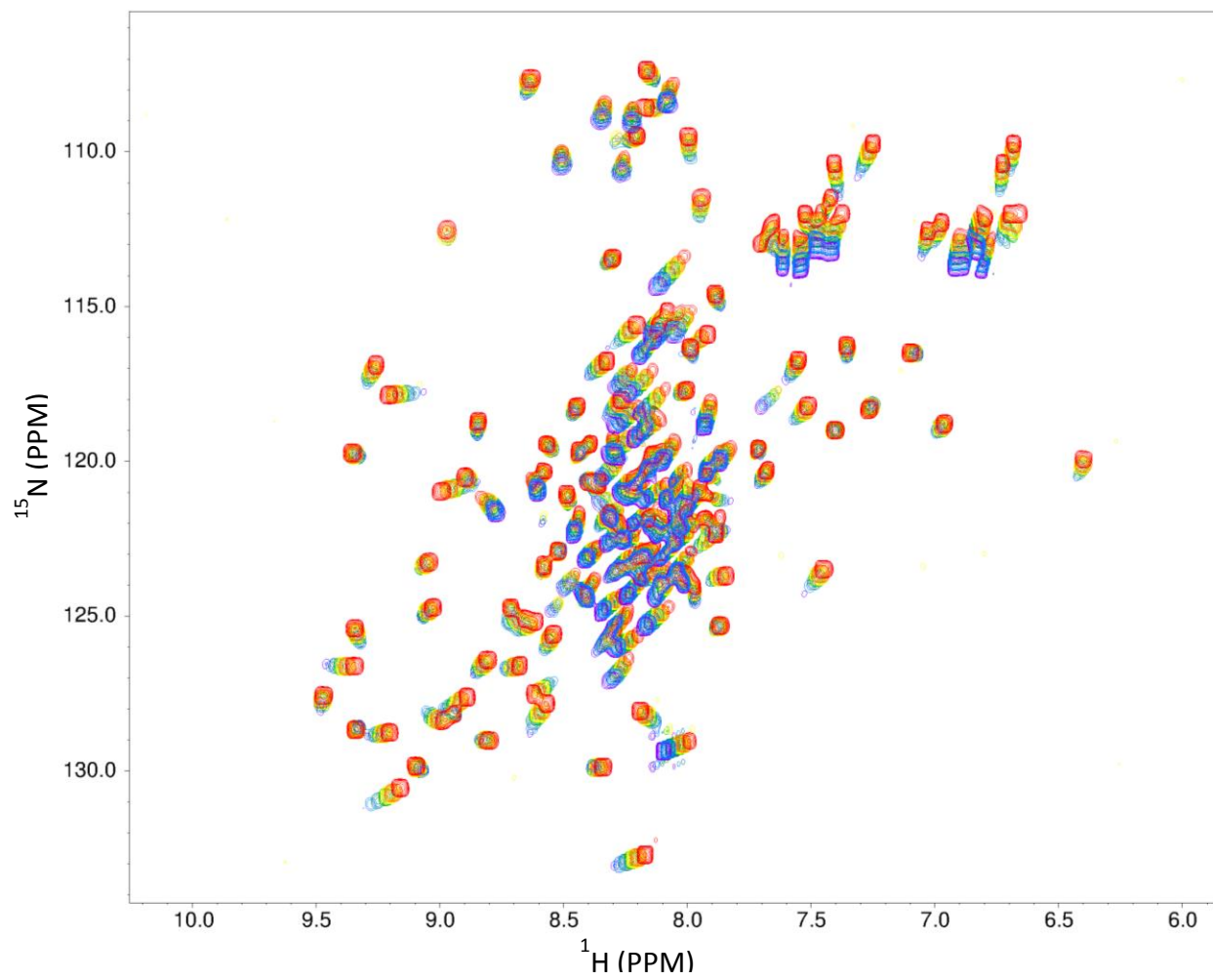


Figure S2. Expanded region of the ZZ-exchange spectrum of CTL9 I98A (Figure 5 in the main text) taken at 600 MHz and 200 ms mixing time for 1 mM  $^{15}\text{N}$  labeled CTL9 I98A in 100 mM NaCl, 20 mM Tris-bis at pH 6.6, 308K and 450 bar.

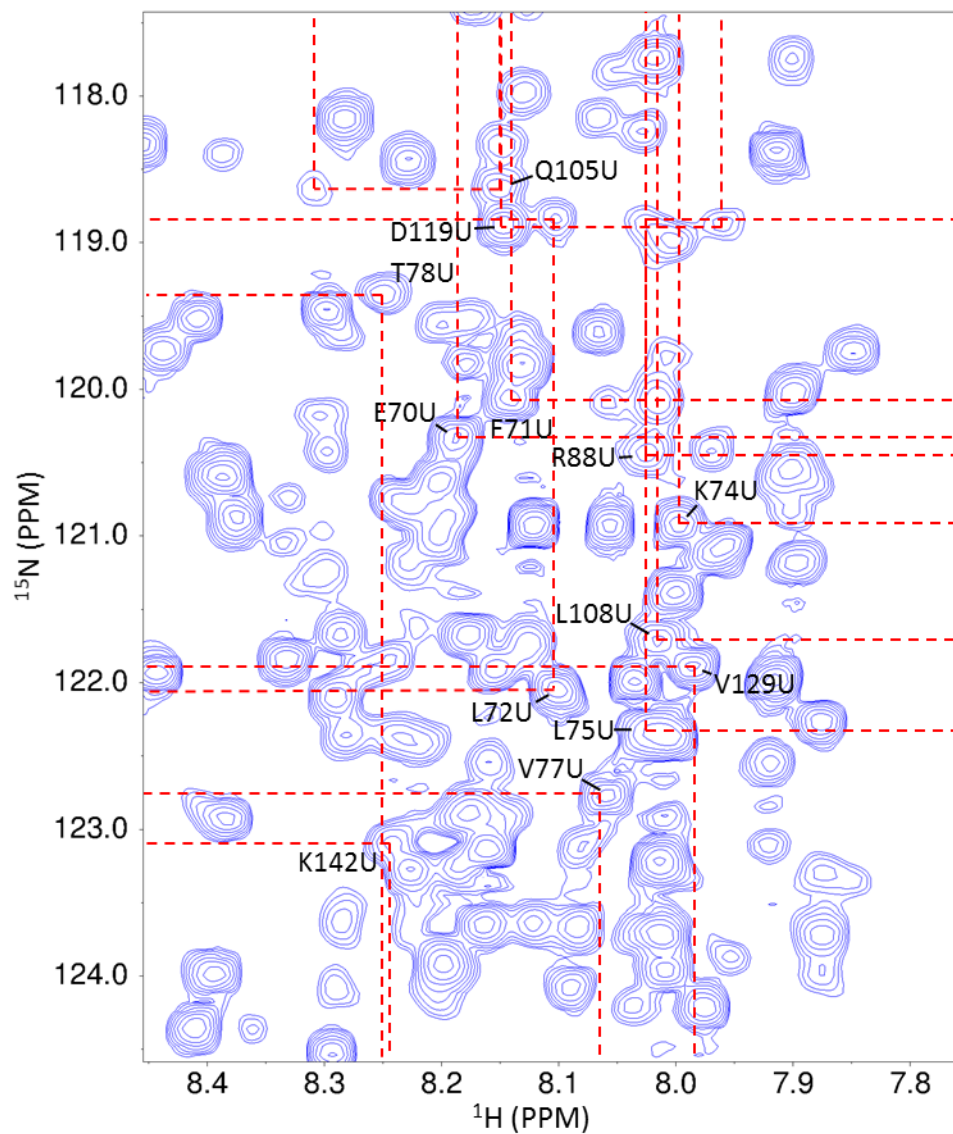
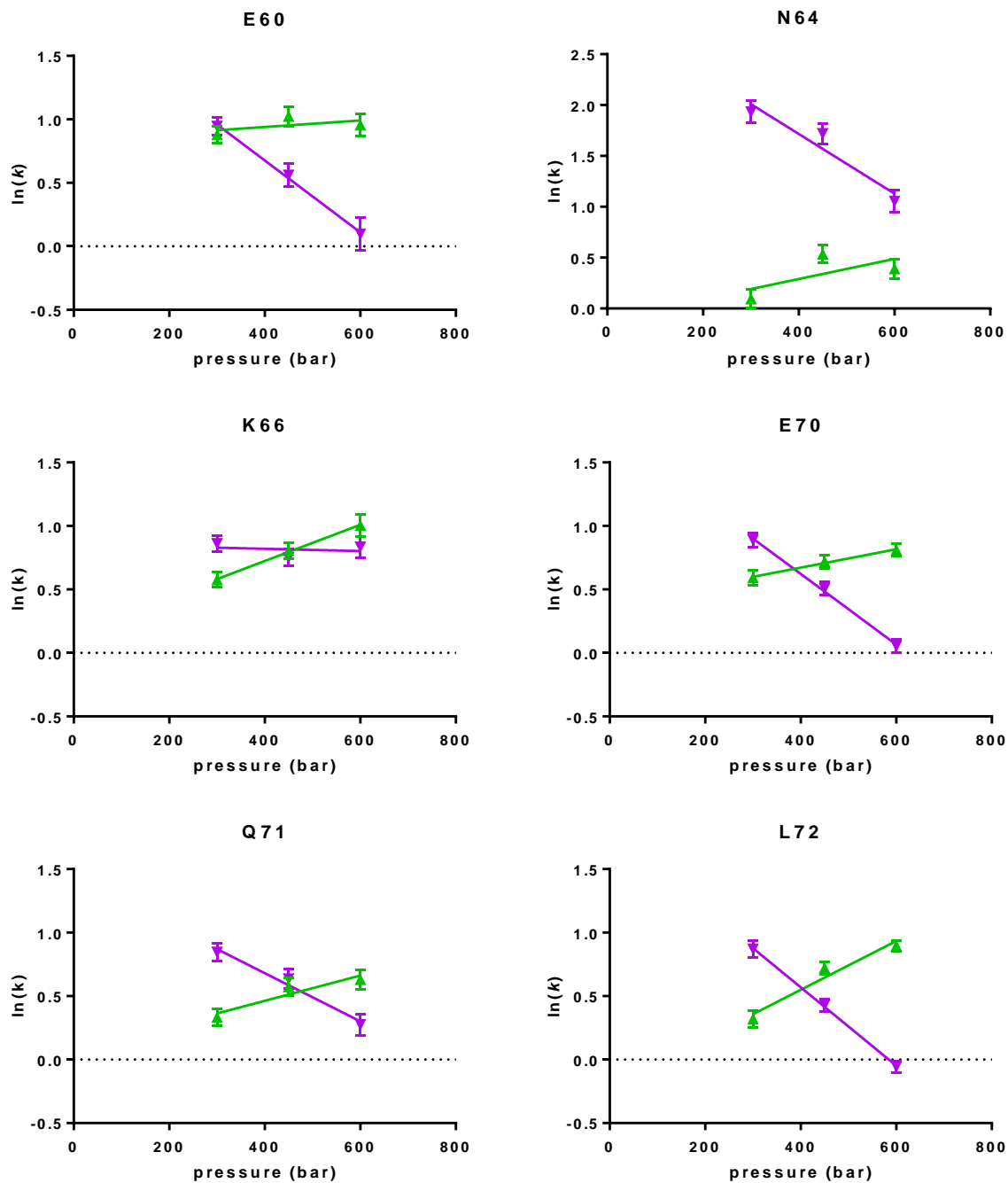
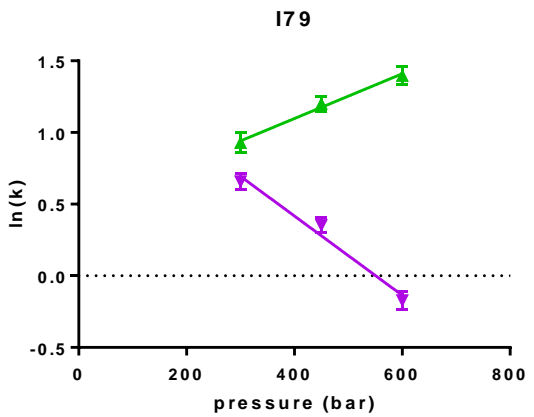
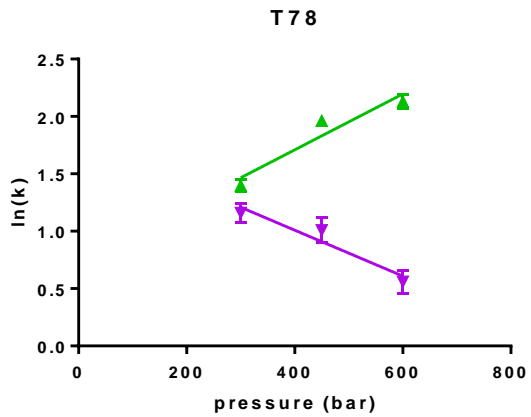
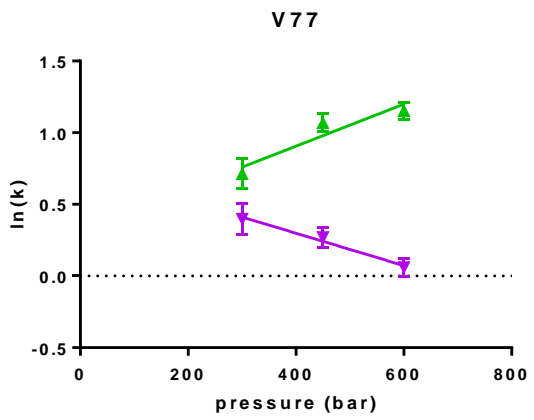
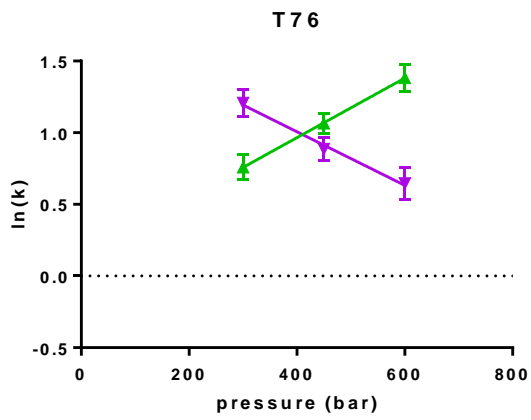
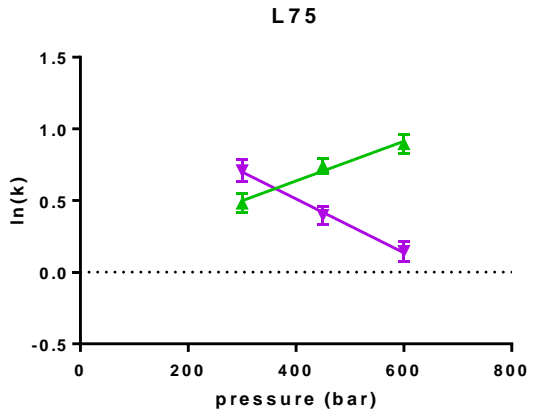
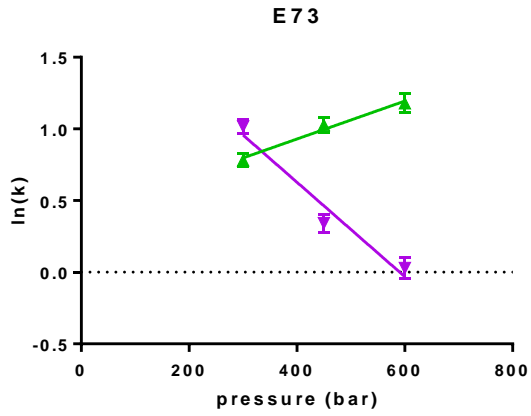
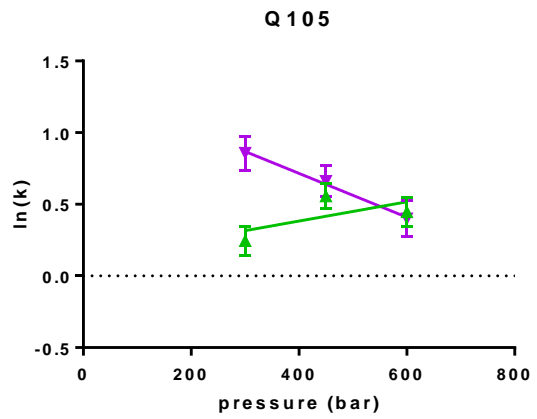
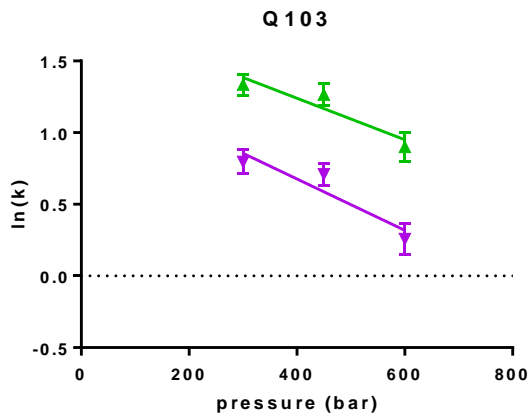
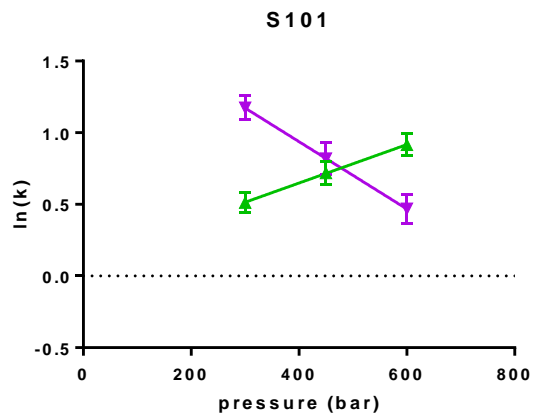
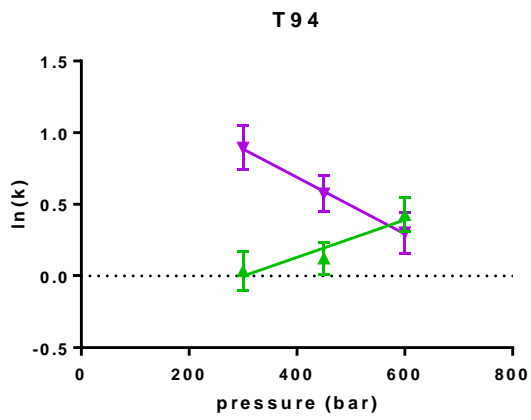
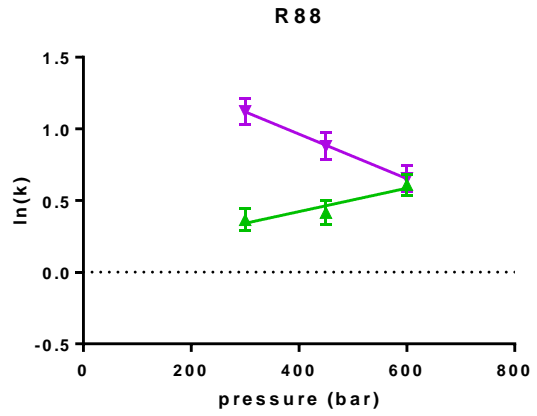
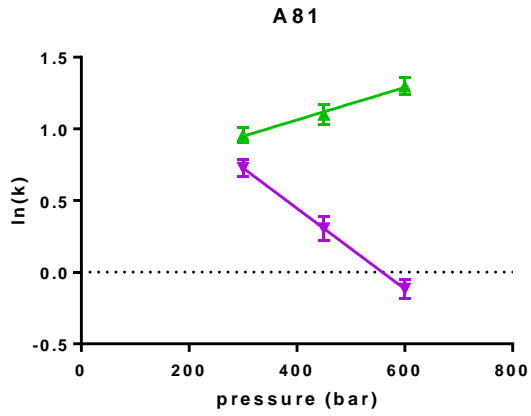
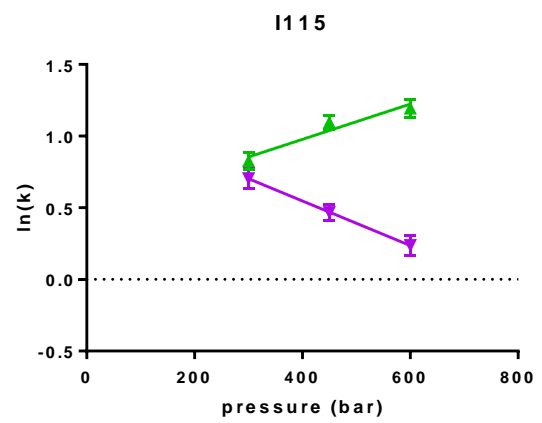
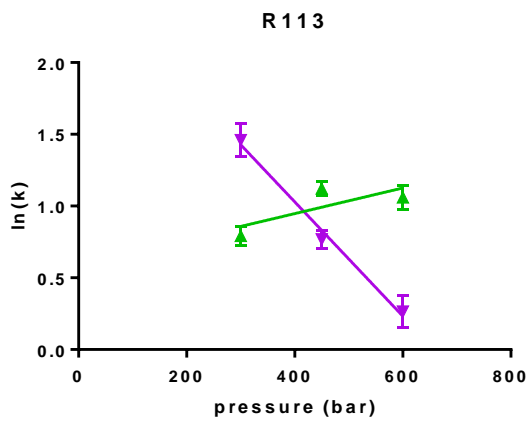
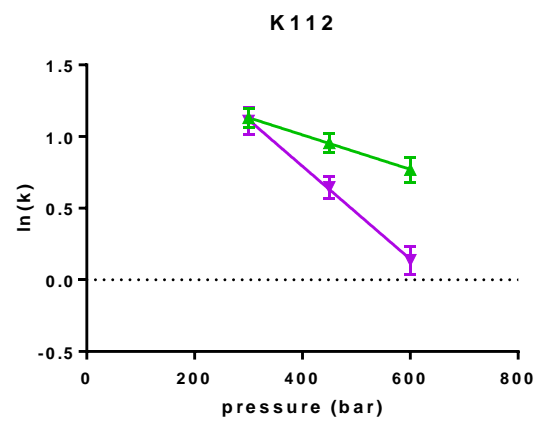
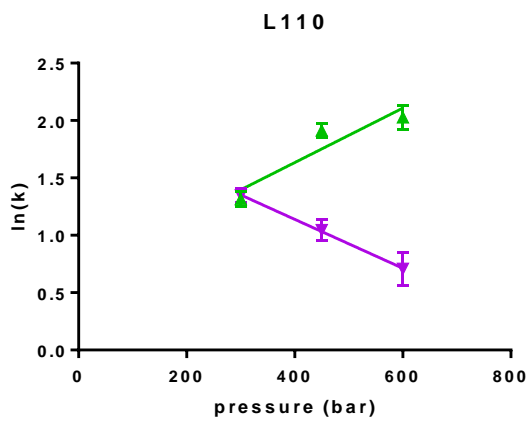
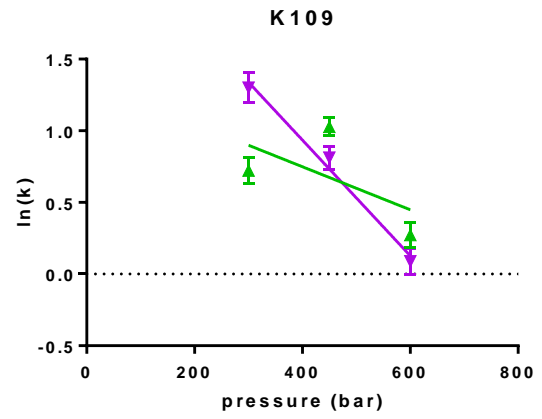
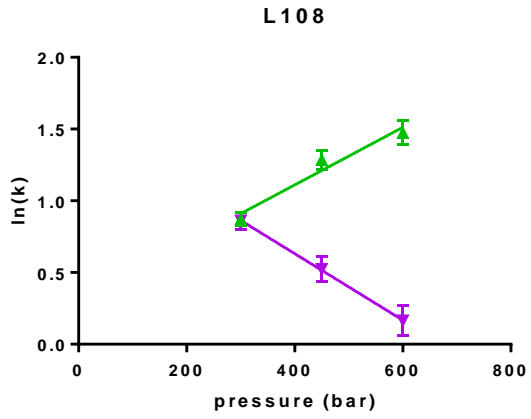


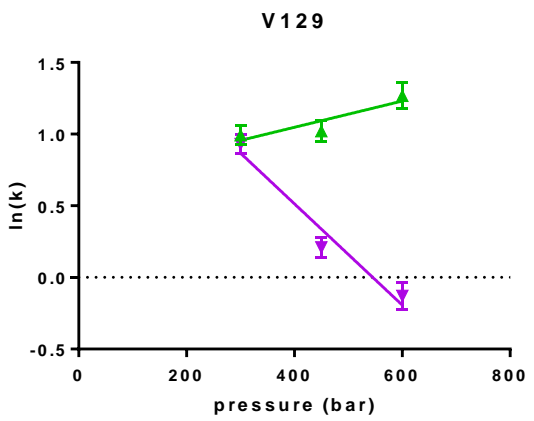
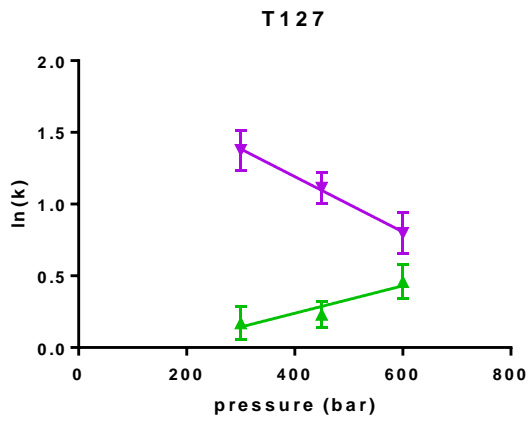
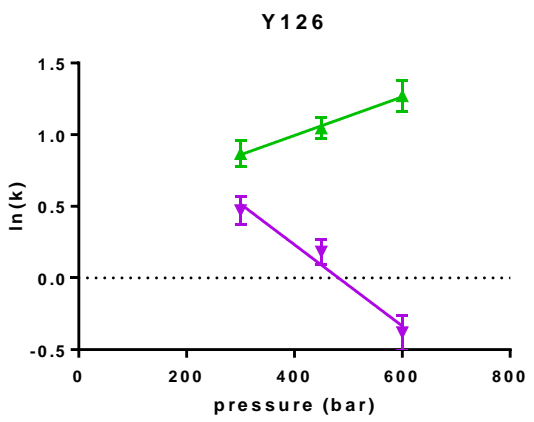
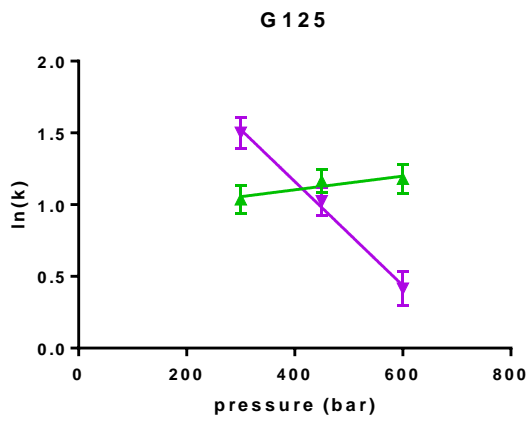
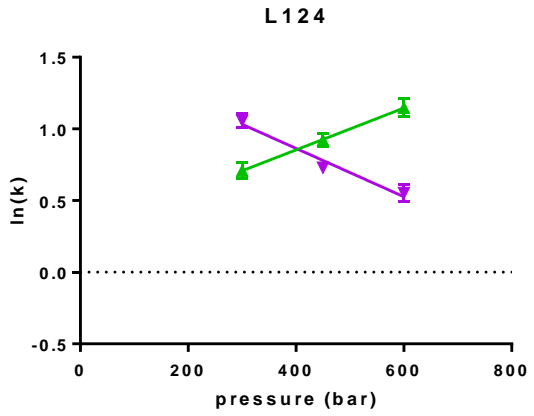
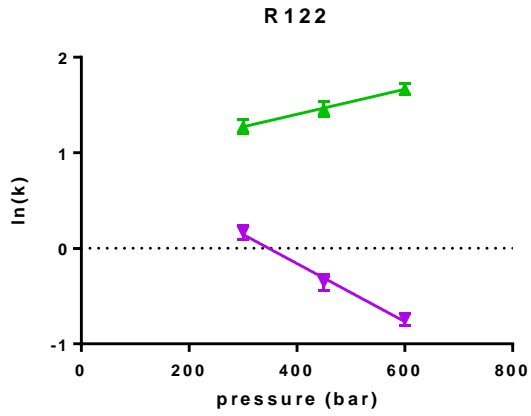
Figure S3. Linear regression of  $\ln(k)$  as a function of pressure obtained from pressure dependent ZZ-Exchange Spectroscopy on CTL9 I98A. The Green data points and lines represent the unfolding rate constant, and the purple data points and lines represent folding rate constants. The residue number is indicated at the top of each plot.



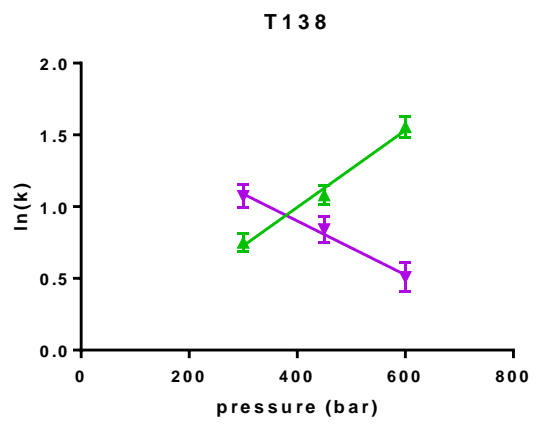
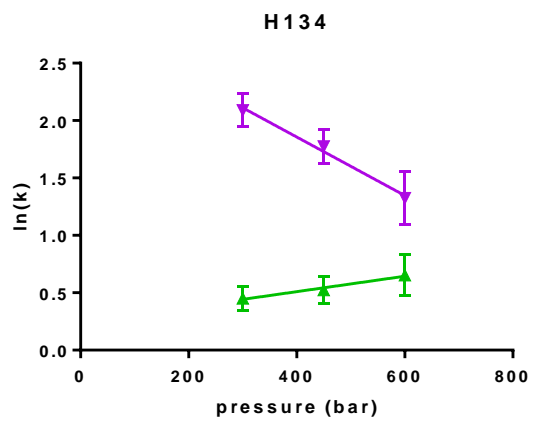
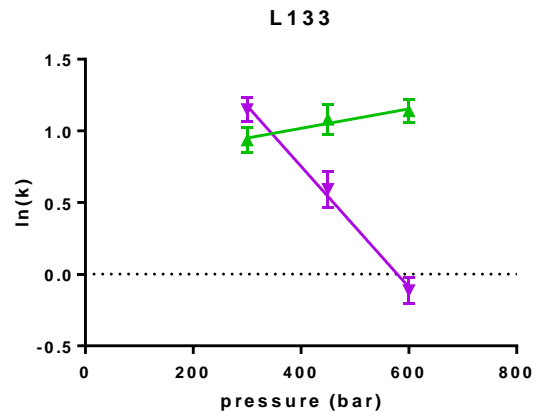
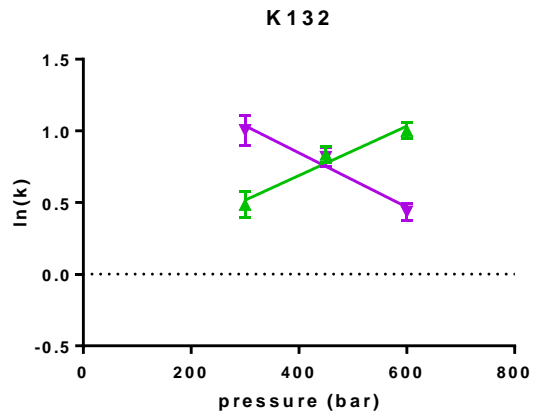


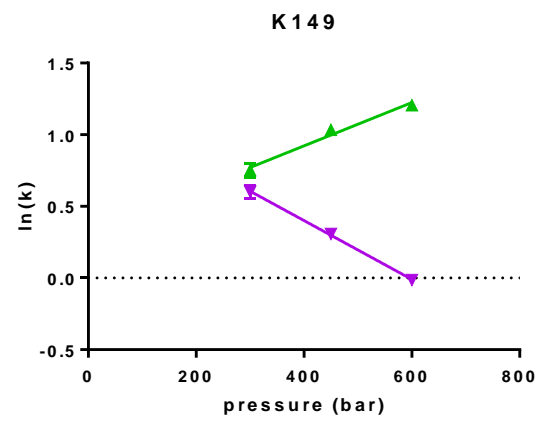
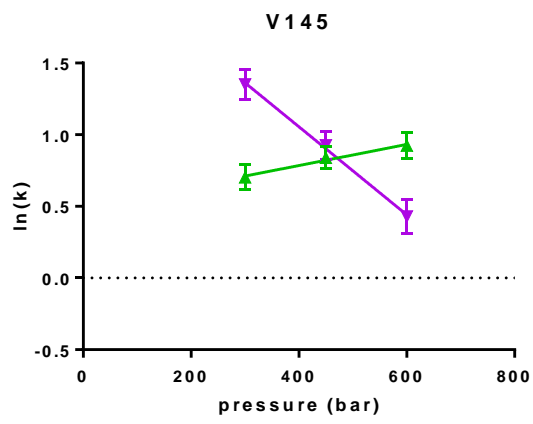
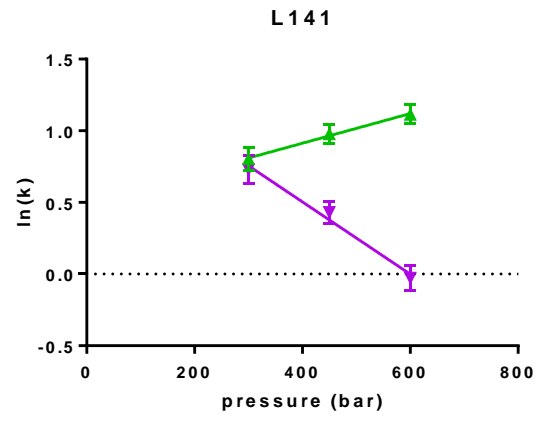
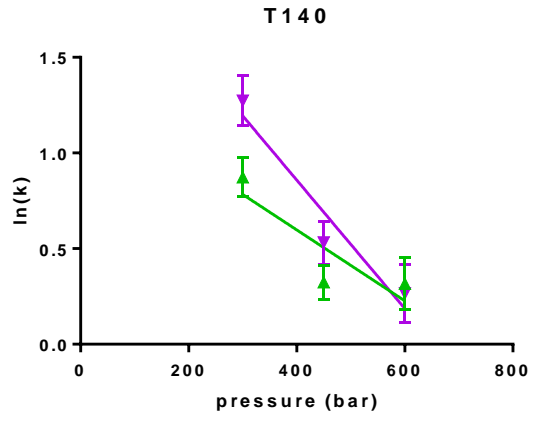












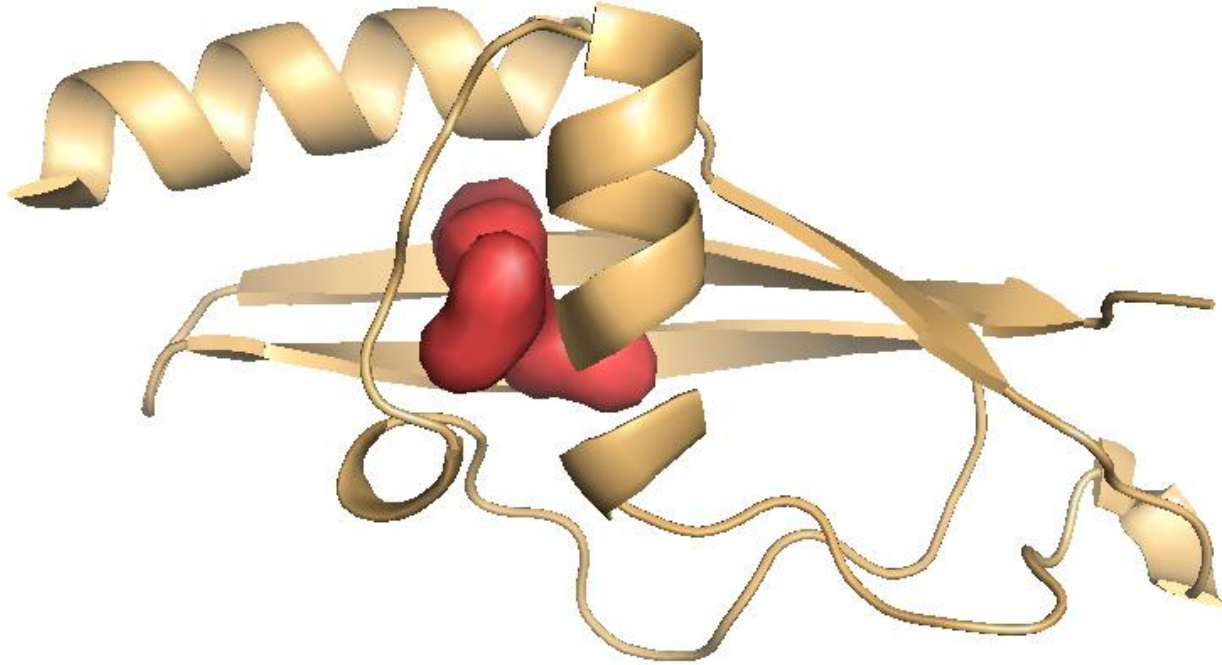


Figure S4. Schematic Ribbon diagram of the structure of CTL9 WT. A large cavity as detected by the software Hollow (<http://hollow.sourceforge.net>) using a probe size of 1.2 Angstroms is depicted as red spheres. The I98A mutation would create a larger cavity in the same region as that depicted here for the WT protein.

Table S1. Residue specific folding rates at atmospheric pressure and activation volumes for CTL9 I98A as described in the text. Only those values for which the uncertainty was less than 30% of the value were retained.

Residue #	$\ln k_f^o$	error	$\Delta V_f^*$	error
60	1.809	0.07117	72.46815	3.907647
64	2.889	0.4037	75.10568	22.16552
70	1.735	0.0643	71.2134	3.531222
71	1.439	0.1365	48.5511	7.492643
72	1.803	0.04023	78.97236	2.209126
73	1.946	0.3245	84.34985	17.81743
75	1.263	0.05307	48.11578	2.91409
76	1.754	0.07367	47.85971	4.045925
77	0.7505	0.07289	28.93605	4.002393
78	1.809	0.2665	51.18863	14.63191
79	1.524	0.1957	70.8549	10.74731
81	1.571	0.003904	72.05843	0.214383
88	1.586	0.01888	39.81907	1.036832
94	1.479	0.04313	50.54845	2.36789
101	1.877	0.004711	60.15113	0.258632
105	1.328	0.05896	39.17889	3.23674
108	1.559	0.01661	59.38291	0.912126
109	2.551	0.2105	103.4016	11.55649
110	1.991	0.03079	54.56877	1.690582
112	2.09	0.0414	83.01828	2.273144
113	2.622	0.1708	101.9676	9.374767
115	1.17	0.004734	39.81907	0.259912
122	1.057	0.1225	77.84564	6.729551
124	1.538	0.1355	43.148	7.441429
125	2.611	0.1192	92.7746	6.54518
126	1.368	0.2478	72.6474	13.60506
127	1.962	0.04725	49.31931	2.594001
129	1.928	0.3433	90.49556	18.90574
132	1.604	0.1758	48.47428	9.653884
133	2.44	0.1349	107.9596	7.40814
134	2.876	0.1202	65.27255	6.598955
138	1.653	0.09106	48.14138	5.001071
140	-	-	86.03993	23.36138
141	1.513	0.1436	64.58115	7.881872
142	1.758	0.08284	62.07166	4.547825
145	2.284	0.06448	78.66507	3.541465
149	1.222	0.0224	52.54581	1.230166
average	1.772473	0.11297	65.44626	6.802498

Table S2. . Residue specific unfolding rates at atmospheric pressure and activation volumes for CTL9 I98A as described in the text. Only those values for which the uncertainty was less than 30% of the value were retained.

Residue #	$\ln k_u^0$	error	$\Delta V_u^*$	error
60	0.8373	0.1939	-	-
66	0.1534	0.02798	-36.5158	1.536683
70	0.3821	0.0321	-18.537	1.762538
73	0.4001	0.08369	-33.8782	4.593917
76	0.1343	0.008987	-53.2116	0.493449
79	0.4726	0.06811	-	-
81	0.6078	0.04712	-29.0897	2.586319
101	0.1119	0.009236	-34.3648	0.507021
103			37.0535	14.58069
112	1.493	0.01191	30.80537	0.65375
115	0.4849	0.1546	-31.5224	8.48876
122	0.8795	0.02472	-33.5197	1.356921
124	0.2697	0.01039	-37.3864	0.570527
125	0.9122	0.09981	-12.2402	5.479924
126	0.456	0.04105	-34.4672	2.253683
127	-	-	-24.5188	8.273661
132	-	-	-44.0955	9.123817
133	0.7465	0.07573	-17.3847	4.158597
134	0.2408	0.04992	-17.2131	2.739962
141	0.4994	0.03203	-26.5034	1.758953
145	0.4907	0.04499	-18.8443	2.470575
149	0.3177	0.1004	-38.6924	5.513213
average	0.585445	0.069109	-23.7063	3.945148